

**Research Article**

## **ELECTROCHEMICAL SYNTHESIS, CHARACTERIZATION AND BIOLOGICAL ACTIVITY OF CHITOSAN METAL COMPLEXES**

**Fikry. M. Reicha<sup>1</sup>, Ayman. S. Shebl<sup>1</sup>, Faried. A. Badria<sup>2</sup> and Ahmed. A. EL-Asmy<sup>3\*</sup>**

<sup>1</sup>Physics Department, Faculty of Science, Mansoura University, Egypt

<sup>2</sup>Pharmacognosy Department, Faculty of Pharmacy, Mansoura University, Mansoura, Egypt

<sup>3</sup>Chemistry Department, Faculty of Science, Mansoura University, Egypt

\*Author for correspondence

### **ABSTRACT**

Copper complexes of chitosan (Cu-CTS) having different copper concentrations were prepared by the electrochemical oxidation technique in aqueous-acetic acid medium (a novel method of preparation) without side reactions. The percentage composition of the complexes was found to depend on the time of electrolysis. All the formed complexes were soluble in the preparation medium indicating that they are charged; probably having positive charges. The properties of these complexes have been demonstrated by partial elemental analysis, spectra (Far-IR; FTIR; UV/Visible spectroscopy, XRD, ESR), swelling studies and thermogravimetric analysis (TGA, DTGA). The IR spectra showed that chitosan behaves in two modes: monodentate and bidentate to form complexes with pendant and bridging models. Their formation (1N, 2N, 3N) seems to be simultaneously occurring where the pendant has the priority while the bridging form is more stable and well separated by replacing the copper anode by platinum to form corresponding complexes (1R, 2R, 3R). The pendant form may be probably formed by ion exchange mechanism, while the bridging by chelation. The electronic spectra showed a maximum wavelength at  $\sim 750$  nm ( $\nu \sim 13300$   $\text{cm}^{-1}$ ) in accordance with octahedral structure which supported by ESR spectra. The amorphous structure of chitosan changed on copper complexes as shown from the XRD patterns. The biological evaluation of the prepared complexes on EAC (Erlich Ascites Carcinoma) and *Vero* cell lines showed that pure chitosan (CTS) and their complexes (1N), (1R), (2R) exhibited an inhibitory effect which reached  $\sim 82\%$ . On the other hand, the prepared samples (2N), (3N) and (3R) showed inhibitory activity 67-70%. The DNA binding affinity assay justified the possible cytotoxic mechanism by showing that (1N) exhibited the highest binding to DNA than that of pure chitosan and the other complexes.

**Key Words:** Chitosan, Electrochemical-oxidation, EAC, DNA affinity

### **INTRODUCTION**

Chitosan, the principal derivative of chitin, is a promising biopolymer material, generally produced by alkaline deacetylation of chitin. Its primary structure is corresponding to a linear chains of  $\beta$  (1-4) linked 2-amino-2-deoxy-D-glucose and 2-acetamido-2-deoxy-D-glucose (Varma, Deshpande, Kennedy 2004). The main parameters that are used for chitosan characterization are deacetylation fraction, molecular weight and crystallinity of biopolymer. When the degree of deacetylation of chitin is higher than 50%, the chitosan becomes soluble in aqueous acidic medium (except dil.  $\text{H}_2\text{SO}_4$ ). Higher deacetylation degree more than 95% is costly and reserved for biomedical applications (Alsarra, Betigeri, Zhang, Evans, Neau 2002). The degree of protonation of amino groups as well as the dissolution in acidic solutions strongly depends on the degree of acetylation of the polymer and neutralization in solution (Sorlier, Deruziere, Viton, Domard, 2001).

Partially N-acetylated chitosan is commercially available. Chitosan and partially acetylated chitosan are more reactive than chitin because they possess OH,  $\text{NHCOCH}_3$  and  $\text{NH}_2$  groups to which metal ions can bind either by chemical or physical adsorption. The presence of a large number of oxygen and nitrogen

## **Research Article**

donors makes the adsorption of metal ions in neutral or moderately acidic media available. However, the  $\text{NH}_2$  groups react much more easily than the OH (Guibal, 2004). Chitosan chelates the metal ions five to six times greater than chitin. This polymer is well known sorbent, effective in the uptake of metal ions, since the amino groups on the chitosan can serve as chelating sites (Juang, Tseng, Wu, Lee 1997). Also, it was shown that the mechanism of metal uptake by chitosan is a combination of adsorption, ion exchange and chelation; the process is complicated and not fully understood (Vold, Varum, Guibal, Smidsrød 2003). Chitosan is effective to form complexes with transition metal ions, but not with alkali and alkaline earth metals (Muzzarelli, Muzzarelli 1998). Adsorption of metal ions takes place using immobilized nitrogenated and oxygenated Lewis bases of chitosan (Cestari, Vieira, Mota, 2008).

Different mechanisms have been suggested to explain the structure of polymer complexes with chitosan. Bridge model, where the metal ions are bound to four nitrogen atoms of either the same or different chains (Juang, Tseng, Wu, Lee 1997; Cestari, Vieira, Mota, 2008; Rhazi, Desbrieres, Tolaimate, Vottero, Alagui, El-Meray 2004). Pendant model where the metal ion is linked to  $\text{NH}_2$  like a pendulum (Braier, Jishi, 2000). Also, the complex was formed having both N and /or O atoms with one or two monomers of the biopolymer (Hernandez, Yala, Merce 2007). The geometries of bridge and pendant models have been analyzed (Lü, Cao, Shen 2008). The results showed that the bridge model is more favorable than pendant model. However, no experimental evidence illustrates the preference of the metal ions to present either as complexes or adsorbed species, or both. In this work we will try to answer upon this remark.

The metal-chitosan binding was found applicable in waste water treatment for heavy metals and radionuclide removal and potable water purification (Babel, Kurniawan, 2003; Dutta, Mohapatra, Ramnani, Sabharwal, Arabinda, Manchanda, 2008; Zhou, Nie, White, He, Zhu, 2009; Tao, Ye, Pan, Wang, Tang, 2009; Papuri, Vijaya, Boddu, Abburi, 2009). Recently, they are promising biomedical agents in many biological applications. Chitosan-Cu(II), Zn(II), Fe(III) or Ag(I) show wide spectrum antimicrobial activity, antifungal, antitumor and low toxicity (Zheng, Yi, Qi, Wang, Zhang, Dyu, 2006; Coleman, Bishop, Booth, Nicholson, 2009; Sanpui, Murugadoss, Pasad, Ghosh, Chattopadhyay, 2008). Association complexes between Cu(II) and Fe(III) showed good candidates as biocompatible catalysis for oxidation or hydrolysis reactions, within wide range of pH (Chiessi, Paradossi, Venanzi, Pispisa, 1992). Complexing abilities of chitosan with Fe(III) have been used to produce low molecular weight of chitosan with narrow- molecular weight distribution (Yin, Zhang, Lin, Feng, Yu, Zhang, 2004). The positive surface charge and compatibility properties of chitosan enable to support cell growth very effectively. Together with the fact that chitosan can be turned into films which are flexible, elastic, and adherent (Ueno, Yamada, Tanaka, Kaba, Matsuura, Okumura, Kadosawa, Fujinaga, 1999). suggest that it may be a suitable matrix for the incorporation of metals for the preparation of long acting antibacterial wound dressing. The search for fields of application of these complexes and development of methods for their production are urgent problems.

In this work, a new method to synthesize Cu-CTS complexes depends on the electrochemical oxidation in acidic-aqueous solution, to avoid the other secondary reactions. Elemental analysis, spectra (IR, UV – Vis, XRD, and ESR) and thermogravimetric analysis are used to confirm the formation of the complexes. Swelling ratio was measured to highlight the physicochemical properties. Also, the biological activity of the prepared complexes was tested.

## **MATERIALS AND METHODS**

### **Materials**

Chitosan with high molecular weight (600,000 g/mol) and degree of deacetylation more than 75% was supplied from Aldrich Chemical Co., acetic acid of analytical grade was purchased from EL-Naser Co., Egypt. The de-ionized water (resistivity  $> 2 \times 10^8 \Omega \text{ cm}$ ) was used for all samples. Copper plates (2 mm, 20 mm, 40 mm) from Sigma- Aldrich of purity 99.995% were well polished using very fine emery paper,

## **Research Article**

cleaned by acetone, ethanol (70 %), and de-ionized water, and used as working electrode (anode) . Platinum rectangular sheet (0.5mm, 20 mm, 40 mm) Sigma-Aldrich and cleaned before used as counter electrode (cathode).

### **Preparation of complexes**

The copper-chitosan complexes were prepared by the electrochemical oxidation of the copper metal in an aqueous acidic medium at constant potential (2 V) using potentiostat. The solutions were prepared by dissolving 1 wt% chitosan into 2% acetic acid, stirred magnetically for 24 h to complete dissolution and to remove the puples, the viscous solution was kept overnight. Copper (anode) and platinum (cathode) plates were immersed in the solution separated by 5 cm and connected to a suitable variable resistor, Picometer (Keithly 485), voltmeter (Keithly 175) and potential power supply (ECOS) at 25 °C with continuous stirring. Nitrogen gas current was flushed into the electrolyte during all the preparation.

The time needed to reach the equilibrium concentration of the metal ion in the solution was accomplished when copper deposited on the cathode (becomes yellowish). The time required to attain the maximum concentration of the copper ions into polymer complex was ~ 5 days. The solution was centrifuged at speed (10000 rpm for 30 min) and filtered to remove any debris. Then divided into two portions, the first designated as Cu-CTS (3N) which contains all possible ions uptake (adsorption and/or chelation) was treated as prepared. However the second was used to differentiate between the types of ion association mechanisms. The main difference between these types of metal uptake is the binding energies in which de-adsorption method was occurring. This process was performed on the solution under investigation electrochemically for another interval of time. This process was carried out by replacing the working electrode (copper) by platinum and the cathode by mirror surface nickel foil (1 mm, 30 mm, 50 mm) under 1.5 V. It was noticed that copper was condensed on the cathode surface and terminated after 2½ days; this complex solution is designated as Cs-Cu (3R). The weight of nickel foil was determined before and after deposition to estimate the percentage of de-ionized metal complexes.

The time attained to prepare low copper concentration complex Cu-CTS (1N) was 10 h, and 2½ days for mild concentration, Cu-CTS (2N), portion of Cu-CTS (2N) was further deionized with the same condition as that of (3N) to prepare the corresponding deionized complex, Cu-CTS (2R). It is worthy to note that, in all cases complex solution did not showed any precipitate, owing to the hydrolysis of copper ions. Similar observation has been reported by (Lü, Cao, Shen, 2008) for complex solutions prepared from their salts (CuCl<sub>2</sub> or FeCl<sub>3</sub>). All the prepared samples were casted onto plastic Petri dishes. The transparent membranes were obtained after drying in air for at least one week and in a vacuum oven at 50 °C for another one week.

### **Physical Measurements**

The weight percentage of chitosan-copper complexes was determined by analysis of their C, H and N content at the Microanalytical Unit of Cairo University. The FTIR spectra were recorded at 25 °C using Mattson 5000 spectrophotometer in the range 4000-400 cm<sup>-1</sup> as: one drop of dilute complex solution was spread on a planar freshly cleavage NaCl plates and held vertically leaving a very thin layer of the material. The solvent was completely removed by pumping at 50 °C for one week. The plates covered by thin film of complexes were introduced to the sample holder of the spectrophotometer. Far-FTIR spectra were recorded using Nicolet spectrometer model 670 , USA, in the region 600-100 cm<sup>-1</sup>, with spectral resolution of 4 cm<sup>-1</sup>; the films of polymer complex were dried at 50° C for one week. The UV/visible spectra were recorded in the 200-800 nm range using ATI Unicom UV/visible vision software V 3.20, at Chemistry Department, Faculty of Science, Mansoura University. The samples of the complexes were prepared as described in IR, quartz plates were used instead of NaCl plates. The plates covered by the thin films were placed in the sample holder of the spectrophotometer. The ESR spectra were recorded at room temperature using a Bruker, EMX spectrometer with microwave power of 25 mw and frequency 9.74 GHz, modulation amplitude of one gauss in the range of 900 -5900 gauss. The sweep time was equal to

## **Research Article**

41.94 s. The X-ray diffraction patterns were obtained using X' Pert Graphics & identify X-ray power diffractometer provided with a diffracted beam monochromator and Cu K $\alpha$  radiation ( $\lambda = 1.5406 \text{ \AA}$ ). The voltage was 40 KV and the current intensity was 30 mA. The  $2\theta$  angle was scanned between  $4^\circ$  and  $40^\circ$ , the XRPD runs carried out at scanning speed of  $2\theta = 2^\circ/\text{min}$ . Film samples (3x4cm) were cut from pure chitosan and copper-chitosan films. Samples with thickness (250-300  $\mu\text{m}$ ) were tested by immersing in a deionized water (pH 7) at room temperature. The sample weights were determined as a function of time after carefully plotting the film with filter paper to remove the adsorbed water on the surface and then weighted immediately on a four digits electronic balance.

Swelling was expressed as the percentage swelled:  $\% \text{Swelling Ratio} = \frac{W_s - W_d}{W_d} \times 100$

Where  $W_s$  is the weight of the dry sample and  $W_d$  is the weight of the wet sample after time  $t$ . Swelling of the chitosan films were investigated at pH 7 and the influence of copper metal ions concentration were evaluated. Thermogravimetric (TGA) analysis and first derivative (DTGA) thermogravimetric analysis were carried out using a Shimadzu TGA-50 H systems. All analyses were performed in platinum cell under a nitrogen atmosphere between 40 and 400  $^\circ\text{C}$ . The experiments were run at a scanning rate of 10  $^\circ\text{C}/\text{min}$ . The relative viscosity measurements were carried out using Ubbelohde viscometer by preparing different concentration of sample and measuring the average time of flow relating to the average time of the same concentration of chitosan itself. By this way relative molecular weight can be estimated.

### **Biological evaluation of copper chitosan samples**

#### **Cytotoxicity**

##### **Sample preparation**

Samples were prepared for assay by dissolving the required amount in 50 ml DMSO and diluting the aliquots into sterile culture medium at 0.4 mg/ml. These solutions were diluted to 0.02 mg/ml in sterile medium and the two solutions were used as stocks to test samples at 100, 50, 20, 10, 5, 2 and 1 mg/ml in triplicate in the wells of 96- microliter plates.

##### **Reagents and cell lines**

RPMI-1640 medium (Sigma Chemical Co., St. Louis, USA). Foetal Bovine serum (GIBCO, UK). Using Ehrlich cells (Erlich Ascites Carcinoma, EAC) were derived from ascetic fluid from diseased mouse (purchased from National Cancer Institute, Cairo, Egypt). The cells were grown in suspension culture, partly floating and partly attached, in RPMI 1640 medium, supplemented with 10% foetal bovine serum. They were maintained at 37  $^\circ\text{C}$  in a humidified atmosphere with 5%  $\text{CO}_2$ . The viability of the cells used in control experiments (DMSO only without drug) exceeded 95% as determined with trypan blue. Tested compounds were prepared initially at concentration 1mg/ml DMSO.

##### **Culture**

Vero African green monkey kidney cells and other cell lines were purchased from Viomed Laboratories, Minnetonka, MN, and grown in Dulbecco's modified Eagle's medium supplemented with 10 % (v/v) calf serum (HyClone Laboratories, Ogden, UT), 60 mg/ml Penicillin G and 100 mg/ml streptomycin sulfate maintained at 37 $^\circ\text{C}$  in a humidified atmosphere containing about 15 % (v/v)  $\text{CO}_2$  in air. All medium components were obtained from Sigma Chemical Co., St. Louis, MO, unless otherwise indicated, Vero stocks were maintained at 34 $^\circ\text{C}$  in culture flasks filled with medium supplemented with 1 % (v/v) calf serum. Subcultures for cytotoxicity screening were grown in the wells of microtiter trays (Falcon Microtest III 96-wells trays, Becton Dickinson Labware, Lincoln Park, NJ) by suspending Cells in medium following trypsin-EDTA treatment, counting the suspension with a hemocytometer, diluting in medium containing 10 % calf serum to  $2 \times 10^4$  cells per 200 ml culture, aliquoting into each well of a tray and culturing until confluent.

## **Research Article**

### **Procedure**

Microtiter trays with confluent monolayer cultures of cells were inverted, the medium shaken out, and replaced with serial dilutions of sterile extracts in triplicate in 100  $\mu$ l medium followed by titrating virus in 100  $\mu$ l medium containing 10 % (v/v) calf serum in each well. In each tray, the last row of wells was reserved for controls that were not treated with compounds. The trays were cultured for 48 hours. The trays were inverted onto a pad of paper towels, the remaining cells rinsed carefully with medium, and fixed with 3.7 % (v/v) formaldehyde in saline for at least 20 minutes. The fixed cells were rinsed with water, and examined visually. Cytotoxicity activity is identified as confluent, relatively unaltered monolayers of stained Cells treated with compounds. Cytotoxicity was estimated as the concentration that caused approximately 50 % loss of the monolayer. DNA as an affinity probe useful in evaluation of biologically active compounds

### **DNA-binding assay**

Analysis of DNA/compound using RP-TLC. TLC plates (RP-18 F 254; 0.25 mm; Merck) were developed with MeOH-H<sub>2</sub>O (8: 2). Test compounds were then applied (5 mg/ml in MeOH) at the origin, followed by the addition of DNA (1 mg/ml in H<sub>2</sub>O and MeOH mixture) at the same position at the origin. The plates were then developed with the same solvent and the position of the DNA was determined by spraying with anisaldehyde. The reagent yields a blue color with DNA and the intensity of the color was proportional to the quantity of DNA added to the plate. Ethidium bromide was used as positive control.

#### *Colorimetric assay*

DNA methyl green (20 mg, Sigma, St. Louis, MO, USA) was suspended in 100 ml of 0.05 M Tris-HCl buffer, pH 7.5, containing 7.5 mM MgSO<sub>4</sub> and stirred at 37 °C with a magnetic stirrer for 24 h. Unless otherwise indicated, samples to be tested were dissolved in EtOH in Eppendorff tubes. Solvent was removed under vacuum and 200  $\mu$ l of the DNA/methyl green solution was added to each tube. The absorbance maxima for the DNA/methyl green complex is 642.5-645 nm. Samples were incubated in the dark at ambient temperature. After 24 h, the final absorbance of samples was determined. Readings were corrected for initial absorbance and normalized as a % of the untreated DNA/methyl green absorbance value. IC<sub>50</sub>'s were determined for each compound.

## **RESULTS AND DISCUSSION**

### **Characterization of copper chitosan complexes**

#### **Elemental analysis**

Elemental analyses of the copper-chitosan (Table 1) showed that the amount of copper ions associated with chitosan increases by increasing the preparation time (i.e. by increasing the dissolution of the anode). The composition% was 1: 17.8 (Cu: glucoseamine unit) for the highly concentrated sample denoted as Cu-CTS (3N), 1: 37.31 for mild Cu-CTS (2N) and 1: 181.8 for low copper concentration, Cu-CTS (1N). After removing the copper ions interacted by physical and/or chemical adsorption (the retended ions are that bonded strongly), the composition was 1: 24.27 for Cu-CTS (3R) and 1: 85.47 for Cu-CTS (2R). However, for low complexed sample, the retended ions were neglected. This proved that the formation of two types of chelation is possible and might simultaneously occur. One may suggest that the copper ions removed in the de-adsorbed process are that bonded in a pendant model. This suggestion may be enhanced by the theoretical calculation (Lü, Cao, Shen, 2008). From Table 1, one can calculate the ratio between the copper ions coordinated as pendant to that bridged. For highly concentrated sample, the ratio is 1: 2.76 and that of mild is 1: 0.77 indicating that the copper ions associated firstly in pendant form with NH<sub>2</sub> groups, may be due to the ion exchange between the H<sup>+</sup> and metal ion M<sup>+</sup> which react much more rapidly than OH (Guibal, 2004).

## Research Article

### FTIR and Far- FTIR spectra

The FTIR spectra of Cu-CTS samples exhibit many alterations from that of CTS as shown in Fig. 1. The major differences are:

1- The broad band centered at  $3420\text{ cm}^{-1}$ , corresponding to the  $\nu(\text{NH}_2)$ ,  $\nu(\text{OH})$  and the hydrated water vibrations, becomes less broadening with increasing the  $\text{Cu}^{+2}$  content in the complexes then the band becomes more narrow indicating more ordered structure. This implies that there is less intermolecular forces within the molecules (Gocho, Shimizu, Tanioka, Chou, Nakajima, 2000).

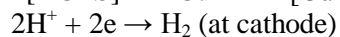
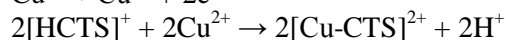
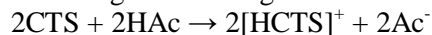
2- The band at  $1550\text{ cm}^{-1}$ , assigned to  $\delta(\text{NH}_2)$  (Caiqin, Ling, Yumin, Xiaowena, Jiaweib, 2002) has maintaining the same position in the complexes but showed a remarkable decrease in intensity, indicating its involvement in complexation.

3- The band at  $1085\text{ cm}^{-1}$  assigned to the second  $-\text{OH}$  group showed a significant shift to lower wave number, as the copper concentration increases suggesting that the second  $-\text{OH}$  group involved in complexation.

4- The band at  $1420\text{ cm}^{-1}$  attributed to  $\delta(\text{OH})$  is shifted to lower wavenumber for (1N) sample, and disappeared in (2N) and (3N) samples, showing that the OH takes part in chelation.

5- The band at  $1637\text{ cm}^{-1}$ , assigned to the  $\nu(\text{C}=\text{O})$  vibration of the amide group, shows no shift in the complexes, but has a significant decrease in intensity as the copper concentration increases, meaning that the CONH group is participated in complexation.

From all the evidence, one can conclude that chitosan bonded with Cu through the  $\text{NH}_2$  in pendant model and through  $\text{NH}_2$  and OH groups in bridged model. The pendant model may proceed through the following ion exchange mechanism:



Strong evidence for the chelation through N and O atoms comes from recording the Far-FTIR spectroscopy which is more significant tool (Cestari, Vieira, Mota, 2008; Sipos, Berkesi, Tomba'cz, Pierre, Webb, 2003). The IR spectra of chitosan has no significant bands in the region  $600\text{-}300\text{ cm}^{-1}$ , however, there are sharp change in the spectra of its complexes. Comparing the spectra of the complexes in this region, one can observe that numerous bands are recorded on complexes having high amount of Cu ions. The spectrum of (3N) complex shows multi defined bands corresponding to the Cu-CTS bonds and assigned to  $\nu(\text{Cu-N})$  in the range  $300\text{-}400$  and  $\nu(\text{Cu-O})$  in the range  $400\text{-}500\text{ cm}^{-1}$  (El-Asmy, Al-Hazmi, 2009). The spectrum of 1N has no bands in the  $300\text{-}400$  region confirming little bonds of Cu with CTS. The broad band at  $525\text{ cm}^{-1}$  is possibly coinciding with the vibrations of HOH) indicating the presence of coordinating water around the Cu ions (aqua-complexes) Table 2 and Fig. 2.

It is more likely to conclude that chitosan- copper complexation occurs primarily through the amino and hydroxyl groups in the sugar unit (Sipos, Berkesi, Tomba'cz, Pierre, Webb, 2003). It is impossible to rule out the participation of  $-\text{OH}$  groups (either from C-6 or C-3) in chitosan complexation since competition of different metal ion (Lewis acidity) can provide the proper conditions for this complexation.

### Spectral studies

The spectrum of chitosan shows a band at  $214\text{ nm}$  due to the amide linkages (El-Asmy, Al-Abdeen, Abo El-Maaty, Mostafa, 2007) as it is the only partially deacetylated chitin. Figure 3 shows two bands in the UV region for Cu-CTS at  $201$  and  $255\text{ nm}$ ; the higher shift is attributed to the complexation of CTS to  $\text{Cu}^{+2}$  (Rahz, Desbrieres, Tolaimate, Rinaudo, Vottero, Alagui, 2002). The band at  $255\text{ nm}$  exhibits some broadening as the amount of copper increases [(2N) and (3N)] than those for de-adsorbed [(2R) and (3R)]. This can be explained by the presence of more than one type of association in as prepared complexes and one type for de-adsorbed one (bridge type).

**Research Article**

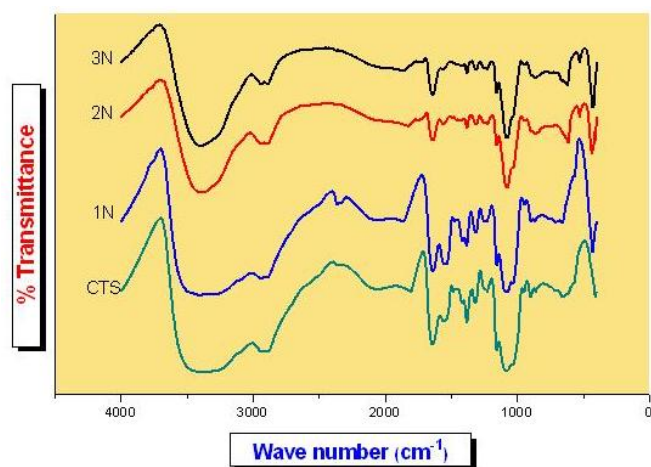


**Figure 1. FTIR spectra of chitosan (CTS) and its complexes samples [(1N), (2N) and (3N)]**

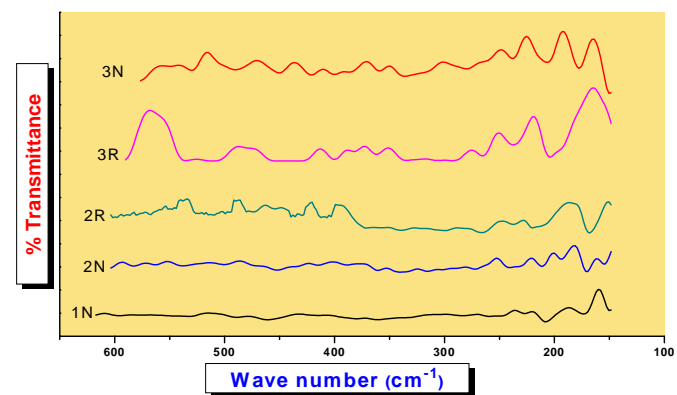


**Figure 2. Far-FTIR spectra of CTS and its complexes samples [(1N), (2N) and (3N)].**

Research Article

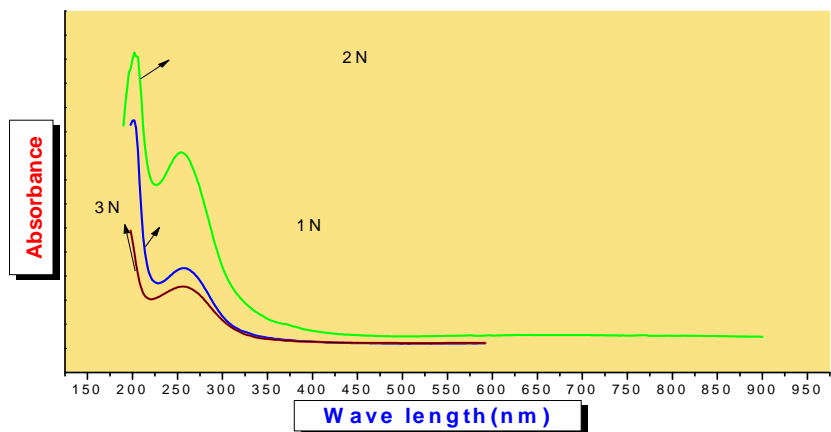


Figure 3a. UV spectra of CTS and its complexes [(1N), (2N) and (3N)]

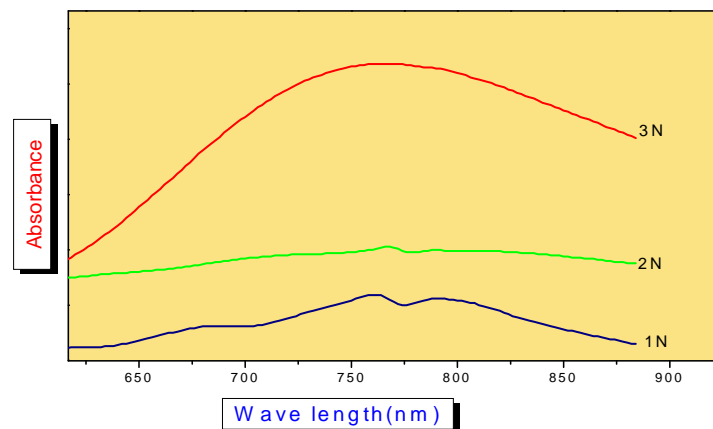


Figure 3b. electronic spectra of CTS and its complexes [(1N), (2N) and (3N)]

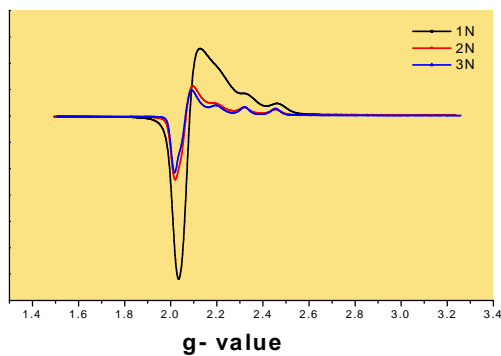


Figure 4. ESR spectra of the complex samples [(1N), (2N) and (3N)]

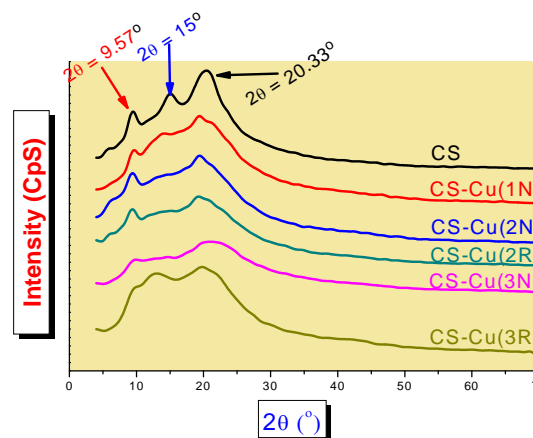


Figure 5. XRD spectra of chitosan (CS) and chitosan-copper complexes



**Research Article**

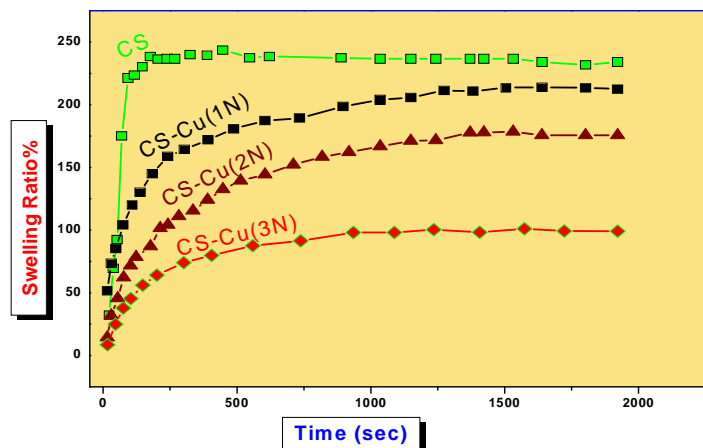


Figure 6. Swelling ratio as function in time (sec)

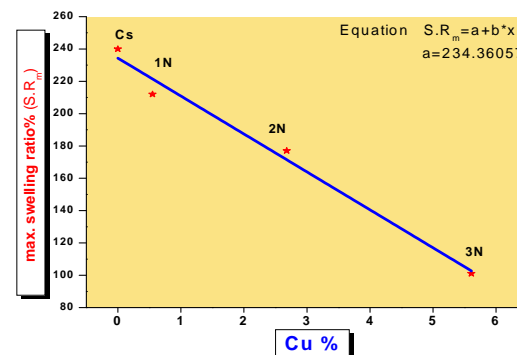


Figure 7: Swelling ratio as function in concentration (sec)

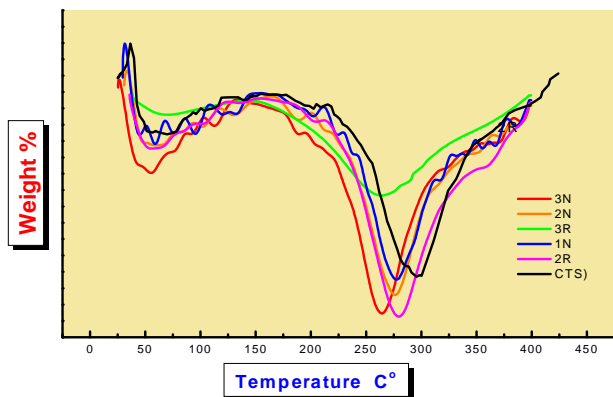


Figure 8. DTGA curves of CTS and its complex samples

Table 1: Element analysis data of CTS and its complexes

Sample	C%	H%	N%	M.R%
CTS	41.19	7.06	6.44	0.83
(1N)	40.01	7.29	6.35	1.38
(2N)	39.99	7.05	6.19	3.51
(2R)	40.67	6.94	6.28	2
(3N)	38.52	6.89	5.44	6.44
(3R)	38.29	7.35	5.58	4.95

**Research Article**

**Table 2: Far FT-IR data of Cu-CTS complexes**

Assignment	CTS	(1N)	(2N)	(3N)	(2R)	(3R)
□HOH aquocomplexe	..... ...	590	580	590		580
□Cu-□□□ complexe	..... ...	505	505	520	501	500
□Cu-OH hydroxyl complexes	..... ....	475	475	478	480	490
□OH aquo complexes	..... ....	428	412	414	422	422

**Table 4: Variation of molecular weight of CTS**

Sample	Molecular Weight (g/mol)
(CTS)	$6 \times 10^5$
(1N)	$5.3 \times 10^5$
(2N)	$4.5 \times 10^5$
(2R)	$2.3 \times 10^5$
(3N)	$1.5 \times 10^5$
(3R)	$1 \times 10^5$

**Table 3: Max. Swelling and time uptake of CTS and its complexes**

Sample	CTS	(1N)	(2N)	(3N)	(2R)	(3R)
Max. swelling	240	207	175	98	192	82
Time uptake	175	1505	1370	935	1538	1109

**Table 5: Thermogravetric data of CTS and its complexes**

	The first Stage		The second Stage	
	Decomposition temperature	Weight loss (%)	Decomposition temperature	Weight loss (%)
CTS	75 °C	4.4	300 °C	41.5
1N	60 °C	8.14	277 °C	41.6
2N	60 °C	8.9	276 °C	41.9
3N	54 °C	9.7	264 °C	41.6
2R	60 °C	6.74	278 °C	41.07
3R	70 °C	5.05	264 °C	40.8

**Research Article**

**Table 6: The cytotoxic activity of chitosan and its complexes against different cell lines**

Compound	Concentration (µg/ml)	(% Viability)			
		HEPGII	WI 38	VERO	MCF 7
CTS (Cu%; 0.0)	25	18	31	40	65
1N (Cu%; 0.55)	25	20	42	48	80
2N (Cu%; 2.68)	25	33	47	38	80
3N (Cu%; 5.61)	25	30	39	42	78
1R (Cu%; 0.14)	25	18	36	46	71
2R (Cu%; 1.17)	25	18	36	46	71
3R (Cu%; 4.12)	25	32	51	52	71

**Table 7: The activity of CTS and its complexes in methyl green/DNA displacement**

DNA-active compounds	DNA/methyl green IC <sub>50</sub> , (mg /ml)*
1N (Cu% ; 0.55 )	58 ± 3
1R (Cu% ;0.14 )	60 ± 1
2N (Cu% ; 2.68 )	62 ± 4
2R (Cu% ; 1.17 )	68 ± 2
3N (Cu% ; 5.61 )	72 ± 2
3R (Cu% ; 4.12 )	70 ± 1
CTS (Cu% ; 0.0 )	74 ± 2

\* Values represent the concentration (mean ± SD, n=3 to 5 separate determinations) required for a 50 %

The electronic spectra in the visible region show a good evidence for the complexation of copper with chitosan. One can observe the absence of any bands for CTS in this region. The Cu-CTS samples have one or two bands at 700-800 nm. Comparing the spectra of 1N, 2N and 3N complexes, it is shown that 1N complex has two bands at 755 and 790 nm while the 3N complex has only on broad band centered at 750 nm. The broadness may be due to the hexa coordination around Cu(II) in the complex having high concentration of copper and resulted from Jahn-Teller effect (Al-Hazmi et al., 2005). The band is assigned to the  ${}^2E_{2g} \rightarrow {}^2T_{2g}$  transition in an octahedral structure (El-Asmy et al., 2010). On the other hand, the 3R complex has two well defined bands.

**ESR spectra**

The spin Hamiltonian parameters and the G values of some of the solid Cu(II) complexes ( $S = 1/2, I = 3/2$ ) are quite similar and displayed an axially symmetric g-tensor parameters with  $g_{\parallel} > g_{\perp} > 2.0023$  indicating that the copper site has a  $d_{x^2-y^2}$  ground-state characteristic of square-planar or octahedral geometry (Al-Hazmi et al., 2005).

The  $Cu^{+2}$  ESR spectra taken at room temperature of the five Cu-CTS samples are shown in Fig.4. These spectra are typically of a well magnetically separated  $Cu^{+2}$  ions. The spectra of the samples (1N), (2N) and (2R) are best resolved, but the spectra of (3N) and (3R) are poorly resolved. It can be noticed that (3R) spectrum is more resolved than (3N), this may be due to the presence of different  $Cu^{+2}$  bonding in (3N)

## Research Article

sample. Also, there are a set of resolved four peaks at low  $g$  – values and broad component structure at the high  $g$  – values. The spectra show no signal of the additional hyperfine structure due to the splitting on nitrogen atoms of the ligands. Analysis of the spectra gave the values of the  $g$  – factors and the hyperfine structure  $g_{11}=2.22348$ ,  $g_{\perp}=2.0443$  and  $A_{11}=180.5$ . These parameters were substituted into the expression:  $g_{av} = [(g_{11}^2 + 2g_{\perp}^2)/3]^{1/2}$  to calculate the  $g_{av} = 2.2234$ . It is clear that  $g_{av} > g_{\perp}$  and  $g_{av} = g_{11}$  characteristic of axial symmetry, which is in agreement with local crystal field of a low symmetry being close to the square – planar coordination (Kramareva, Finashina, Kucherov, Kustov, 2003). EPR spectra with identical HFS parameters (Chiessi et al., 1995) of the ESR spectrum of the complexes suggests a typical elongated octahedral geometry (El-Asmy, Al-Abdeen, Abo El-Maaty, Mostafa, 2010). The small  $g_{11}$  values indicate strong interaction between the ligand and the metal ion.

### X- ray diffraction

The morphology of the Cu-CTS complexes was studied in a facile manner by XRD, which afforded an easy tool to evaluate the extent of binding. Thus a study of XRD is in itself a powerful tool to study the extent of metal binding by polymer ligand where the key functional groups are extensively utilized in binding, thereby disrupting the original polymer structure and the consequent changes in the XRD spectra. Figure 5 shows the XRD patterns of chitosan and Cu-CTS complexes (1N), (2N), and (3N) and that of de-adsorbed (2R) and (3R). The diffractograph of chitosan consists of three characteristic broad peaks at  $2\theta = 9.57$ ,  $15$  and  $20.33^\circ$  come from the amorphous region as reported in literature (Webster, Halling, Grant, 2007). while the characteristic crystalline peaks, usually appear at  $2\theta > 20^\circ$  are absent in these samples. This is in agreement with the reported results (Yin, Zhang, Lin, Feng, Yu, Zhang, 2004; Ogawa, 1991) in which, they referred the degree of crystallinity to its degree of deacetylation and molecular weight. Higher degree of deacetylation lower molecular weight arises to higher degree of crystallinity. The Peak observed at around  $15^\circ$  has been attributed to the anhydrous crystal lattice (Ogawa, 1991. Moreover, peak in the range 9-13 refers usually to disordered portions of the polymer in the C-2 amino group (Ogawa, 1991). The second broad region from  $2\theta = 10 - 23^\circ$  are attributed to the hydrophilic pockets in the polymer, i.e. a hydroxyl alcohols from both C6 and the glucosamine monomeric ring structure and amide groups on the backbone of chitosan.

The diffractograph of (3N) sample shows that the first broad signal in the XRD of chitosan disappeared indicating that the copper ions are complexed as a bridge model. The second peak at  $2\theta = 15^\circ$  in chitosan is also disappeared, while the intensity of the signal at  $2\theta = 20.33^\circ$  is reduced and broaden. This is a clear indication that a great deal of these copper ions favors interaction with the amorphous region of chitosan (Schmuhl, Kreig, Kiezer, 2001) to form bridge involving  $NH_2$  and OH groups and pendant or absorbed in the amorphous pockets. The diffractograph of (3R), formed by de-absorption of copper ions in the (3N) sample, showed that, the signal at  $2\theta = 9.57^\circ$  still disappearing, with the appearance of a broad peak at  $2\theta = 15^\circ$ . The pockets and the peak at  $2\theta = 20.33^\circ$  become narrow. This indicates that the decomplexation of the weak bonding sites of amorphous pockets and the associated copper ions by bridging with  $NH_2$  groups is stronger than that corporate by pendant or absorption.

The XRD pattern of (2N) and (1N) and those of corresponding de adsorbed (2R) and (1R) showed that the position of amorphous peaks unaltered while their intensities and broadening affected. Summarizing the XRD data, the peak at  $9.57^\circ$  is attributed to  $NH_2$  groups, while that at  $15^\circ$  is due to the anhydrous crystal lattice. Moreover, a significant conclusion is the presence of two coordination possibilities of copper ions with chitosan and the bridge model is the most stable.

### Swelling studies

Figure 6 shows the swelling% of CTS and Cu-CTS films as a function of time. The profiles obtained show that CTS imbibing up to maximum swelling 240% of its own weight and as the copper ions concentration increase in the sequence Cs-Cu (1N), Cs-Cu (2N) and Cs-Cu (3N), one can observe that:

## Research Article

- 1- The swelling rate has an exponential behavior represented by the following equation:

$$S.R_{(t)} = S.R_{(m)} - ce^{-dt}$$

Where  $S.R_{(t)}$  : represents the swelling ratio at time (t) and  $S.R_{(m)}$  : represents the maximum swelling ratio.

- 2- The maximum swelling decreases linearly with copper ion concentration (Fig. 7), expressed by the following equation:

$$S.R_{(m)} = a - b*(Cu \%).$$

- 3- The time uptake of water decreases as the copper ions concentration increases (Table 3). This may be attributed to that the copper ions act as cross-linker between chitosan chains, thus producing cross-linked points in the polymeric chains and increase the extent of cross-linking of the polymer network, which reduce water polymer hydrogen bonds and reducing the chain mobility. These results agree with reports by (Lopez, Bodmeier, 1997) who suggested that the extent of swelling was less in cross-linked films. De-ionized samples (2R) and (3R) differ slightly than their corresponding as prepared ones in maximum swelling values.

### Relative viscosity measurement

The influence of average molecular weight (Mw) on the viscosity development of aqueous solutions plays an important role in the application of chitosan. By measuring relative viscosity of chitosan and chitosan copper complex solutions as shown in (table 4), we found that; the relative viscosity of chitosan and chitosan copper complexes decreases as the elctro-oxidation time increases. This could be attributed to degradation of the chain. This part is very important and need further work.

### Thermogravimetric analysis (TGA, DTGA)

The thermogravimetric (TGA) curves (Fig. 8) for CTS and Cu-CTS complexes show that the degradation of CTS took place in three steps at 75, 101 and 300 °C with weight loss of 4.4% for the first two steps and 41.4% for the last step. The result is similar to that reported (Neto, Giacometti, Job, Ferreira, Fonseca, Pereira, 2005) where the first two steps are assigned to the loss of the hydrated and bonded water. The third step is corresponding to the decomposition of chitosan, vaporization and elimination of volatile moieties.

The polymer complexes (1N, 2N and 3N) and the corresponding (1R, 2R and 3R) complexes are degraded in two steps. It is clearly seen from Fig. 8 and Table 5 that, as the concentration of copper ions increases the start temperature of the decomposition decreases and the weight of water loss increases reaching optimum for the most concentrated complex (3N). An examination of the DTG curve of (3N) shows splitting of the major degradation peak corresponds to water loss to four weak decomposition peaks. According to these results, one can conclude that, the water in (3N) is generally classified into four different thermal species: freezable water, water associated with copper ions which bonded with NH<sub>2</sub> and OH groups in pendant model and that chelated in a bridging form with the same or different functional groups with thermal stability increases in the same sequences. The results of comparative study of interaction of copper ions and chitin and chitosan by density functional calculation (Lü, Cao, Shen, 2008) as well as other experimental results (Neto, Giacometti, Job, Ferreira, Fonseca, Pereira, 2005) support these data.

Furthermore, comparing the DTG curve of (3R) with (3N), one can clearly see the disappearance of these weak peaks , the peak area decreased markedly and become smoothed asymmetric one extended to higher temperature, this peak starts at 40 °C ended at 134 °C. So, one can believe that the weight loss is due to freezable water and that chelated in a bridging form with the same or different two functional groups. The second decomposition stage shows no change in the decomposition temperature indicating that they have the same thermal stability. We can conclude that, the DTGA data ensure the removal of copper ions which bonded with -NH<sub>2</sub> or -OH groups in pendant form.

Biological evaluation of copper chitosan complexes

## Research Article

### Cytotoxicity

The results of cytotoxic assay table 6 showed that chitosan and its complexes (1N, 1R and 2R) exhibit an inhibitory effect in the range 80-82%. On the other hand, the complexes (2N, 3N and 3R) showed inhibitory activity in the range of 67-70%. This may be attributed to the possible model of action that chitosan and (1R and 2R) have the  $\text{NH}_3^+$  groups free (as a result of decomposition of pendant model).

### DNA-binding assay

The copper complexes interact with DNA, leading to chemically induced cleavage of DNA and thus, antitumor activity. The mode of action is probably related to the binding of chitosan and copper, which is likely to leave some potential donors free and these free donors enhance the biological activity [19]. The DNA binding affinity assay justified the possible mechanism of the tested compounds against cell lines. The data in Table 7 show that (1N) complex exhibits the highest binding to DNA than chitosan and its complexes. This may be related to the possible interaction of  $\text{Cu}^{2+}$  with  $\text{NH}_3^+$  in pendant model more than bridged model. The activity decreases in the order:

$1\text{N} > 1\text{R} > 2\text{N} > 2\text{R} > 3\text{R} > 3\text{N} > \text{CTS}$

The highest value recorded in 1N may be attributed to the presence of more positive charge on pendant model,  $[\text{Cu-CTS}]^{2+}$ , than  $\text{HCTS}^+$  which interact readily with the negatively charged substances at the cell surface of the organism; the highest positive charge density enhanced its adsorption.

### ACKNOWLEDGEMENTS

The authors would like to acknowledge the effort of Prof. Dr. M. Hefni (Assuit University) for helping in interpreting the results obtained by ESR. The authors also thank the Post Graduates and Research Department at Mansoura University for their financial support.

### REFERENCES

- Al-Hazmi GAA, El-Shahawi MS, Gabr IM, El-Asmy AA (2005).** Spectral, magnetic and electrochemical studies on new copper(II) thiosemicarbazone complexes. *Journal of Coordination Chemistry* **58** (8) 713.
- Alsarra IA, Betigeri SS, Zhang, Evans HB, Neau SH (2002).** Molecular weight and degree of deacetylation effects on lipase-loaded chitosan bead characteristics. *Biomaterials* **23** 3637–3644.
- Babel S, Kurniawan TA (2003).** Low - cost adsorbents for heavy metals uptake from contaminated water; a review. *Journal of Hazardous Material* **97** 219-243.
- Braier NC, Jishi RA (2000).** Density functional studies of  $\text{Cu}^{+2}$  and  $\text{Ni}^{+2}$  binding to chitosan. *Journal of Molecular Structure* **49** 951–55.
- Caiqin Q, Ling X, Yumin D, Xiaowena S, Jiaweib C (2002).** A new cross-linked quaternized-chitosan resin as the support of borohydride reducing agent. *Journal of Reactive & Functional Polymers* **50** 165–171.
- Cestari AR, Vieiraa EFS, Mota JA(2008).** The removal of an anionic red dye from aqueous solutions using chitosan beads-The role of experimental factors on adsorption using a full factorial design. *Journal of Hazardous Materials* **160** 337-343.
- Chiessi E, Branca M, Palleschi A, Pisisa B (1995). Copper(II) Complexes Immobilized on a Polymeric Matrix. *Journal of Inorganic Chemistry* **34** 2600-2609.
- Chiessi E, Paradossi G, Venanzi M, Pispisa B (1992).** Copper Complexes Immobilized to Chitosan. *Journal of Inorganic Biochemistry* **46** 109-118.
- Coleman NJ, Bishop AH, Booth SE, Nicholuson JW (2009).**  $\text{Ag}^+$  and  $\text{Zn}^{2+}$  - exchange kinetics and antimicrobial properties of  $11\text{\AA}$  tobermorites. *Journal of European Ceramic Society*, **29** 1109–1117.
- Dutta S, Mohapatra PK, Ramnani SP, Sabharaeal S, Arabinda KD, Manchanda VK (2008).** Use of chitosan derivatives as solid phase extractors for metal ions. *Journal of Desalination* **232** 234-242.

## **Research Article**

**El-Asmy AA, Al-Abdeen AZ, Abo El-Maaty WM, Mostafa MM (2010).** Synthesis and spectroscopic studies of 2,5-hexanedione bis(isonicotinylhydrazone) and its first row transition metal complexes. *Journal of Spectrochimica Acta A* **75** 1516.

**El-Asmy AA, Al-Hazmi GA A (2009),** Spectral features of benzophenone substituted thiosemicarbazones and their Ni(II) and Cu(II) complexes. *Spectrochimica Acta A* **71** 1885-1890.

**Gocho H, Shimizu H, Tanioka A, Chou TJ, Nakajima T (2000).** Effect of polymer chain end on sorption isotherm of water by chitosan. *Journal of Carbohydrate Polymers* **41** 87–90.

**Guibal E (2004).** Interactions of metal ions with chitosan-based sorbents: a review. *Separation and Purification Technology* **38** 43–74.

**Hernandez RB, Yala OR, Merce ALR (2007).** Chemical Equilibrium in the complexation of first transition series divalent cations Cu<sup>2+</sup>, Mn<sup>2+</sup> and Zn<sup>2+</sup> with chitosan. *J. Brazilian Chemical Society* **18** 1388-1396.

**Juang RS, Tseng RL, Wu FC, Lee SH (1997).** Adsorption Behavior of Reactive Dyes from Aqueous Solutions on Chitosan. *J. Chem. Technol. Biotechnol*, **70** 391-399.

**Kramareva NV, Finashina ED, Kucherov AV, Kustov LM (2003).** Copper Complexes Stabilized by Chitosans: Peculiarities of the Structure, Redox, and Catalytic Properties Kinetics and Catalysis. *Journal of Kinetics and Catalysis* **144** 793-800.

**Lima IS, Airoidi C(2004).** A thermodynamic investigation on chitosan–divalent cation interactions. *Journal of Thermochemica Acta* **421** 133-139.

**Lopez CR, Bodmeier R (1997).** Mechanical, water uptake and permeability of crosslinked chitosan glutamate and alginate films. *Journal of Controlled Release* **44** 215-225.

**Lü R, Cao Z, Shen G (2008).** Comparative study on interaction between copper (II) and chitin/chitosan by density functional calculation. *Journal of Molecular Structure* **860** 80-85.

**Muzzarelli RAA, Muzzarelli B (1998).** In *Polysaccharides* (Ed. S. Dimitriu, Marcel Dekker) New York, Chapt 17.

**Neto CGT, Giacometti JA, Job AE, Ferreira FC, Fonseca JLC, Pereira MR (2005).** Thermal analysis of chitosan based networks. *Journal of Carbohydrate Polymers* **62** 97–103.

**Ogawa K (1991).** Effect of heating and aqueous suspension of chitosan on the crystallinity and polymorphs. *Agriculture and Biological Chemistry* **55** 2375-2379.

**Papuri SR, Vijaya Y, Boddu VM, Abburi K (2009).** Adsorptive removal of copper and nickel ions from water using chitosan coated PVC beads. *Journal of Bioresource Technology* **100** 194-199.

**Rhazi M, Desbrieres J, Tolaimate A, Vottero P, Alagui A, El- Meray M (2002).** Influence of the nature of the metal ions on the complexation with chitosan. Application to the treatment of liquid waste. *Journal of European Polymer* **38** 1523-1530.

**Rahzi M, Desbrieres J, Tolaimate A, Rinaudo P, Vottero P, Alagui A (2002),** Contribution to the study of the complexation of copper by chitosan and oligomers. *Polymer* **43** 1267-1276.

**Sanpui P, Murugadoss A, Pasad PVD, Ghosh SS, Chattopadhyay A (2008).** The antibacterial properties of a novel chitosan – Ag - nanoparticle composite. *International Journal of Food Microbiology* **124** 142- 146.

**Schmuhl R, Kreig HM, Kiezer K (2001).** Adsorption of Cu(II) and Cr(VI) ions by chitosan. *Water* **27** 1-7.

**Sorlier P, Deruziere, Viton AC, Domard A (2001).** Relation between the degree of acetylation and electrostatic properties of chitin and chitosan. *Biomacromolecules* **2** 765-772.

**Sipos P, Berkesi O, Tomba'cz E, Pierre TGS (2003).** Formation of spherical iron oxyhydroxide nanoparticles sterically stabilized by chitosan in aqueous solutions. *Journal of Inorganic Biochemistry* **95** 55-63.

**Tao Y, Ye L, Pan J, Wang Y, Tang B (2009).** Removal of Pb(II) from aqueous solution on chitosan/TiO<sub>2</sub> hybrid film. *Journal of Hazardous Material* **161** 718- 722.

**Research Article**

**Ueno H, Yamada H, Tanaka I, Kaba N, Matsuura M, Okumura M, Kadosawa T, Fujinaga T (1999).** Accelerating Effects of Chitosan for Healing at Early Phase of Experimental Open Wound in Dogs. *Journal of Biomaterials* **20** 1407-1414.

**Varma AJ, Deshpande SV, Kennedy JF (2004).** Metal complexation by chitosan and its derivatives: a review. *Carbohydrate Polymers* **55** 77–93.

**Vold IM, Varum KM, Guibal E, Smidsrqd O (2003).** Binding of ions to chitosan – selectivity studies. *Journal of Carbohydrate Polymer* **54** 471 - 477.

**Webster A, Halling MD, Grant DM (2007).** Metal complexation of chitosan and its glutaraldehyde cross-linked derivative. *Carbohydrate Research* **342** 1189-1201.

**Yin X, Zhang X, Lin Q, Feng Y, Yu W, Zhang Q (2004).** Metal-coordinating controlled oxidative degradation of chitosan and antioxidant activity of chitosan-metal complex. *ARKIVOC* 66-78.

**Zheng Y, Yi Y, Qi Y, Wang Y, Zhang W, Dyu M (2006).** Preparation of chitosan – copper complexes and their antitumor activity. *Bioorganic & Medicinal Chemistry Letters* **16** 4127- 4129.

**Zhou YTH, Nie L, White CB, He ZY, Zhu LM (2009).** Removal of Cu<sup>2+</sup> from aqueous solution by chitosan-coated magnetic nanoparticles modified with  $\alpha$ -ketoglutaric acid. *Journal of Colloid and Interface Science* **330** 29-37.